

Supplemental Information

NF- κ B Shapes Metabolic Adaptation by Attenuating Foxo-mediated Lipolysis in *Drosophila*

Maral Molaei, Crissie Vandehoef, and Jason Karpac

Figure S1

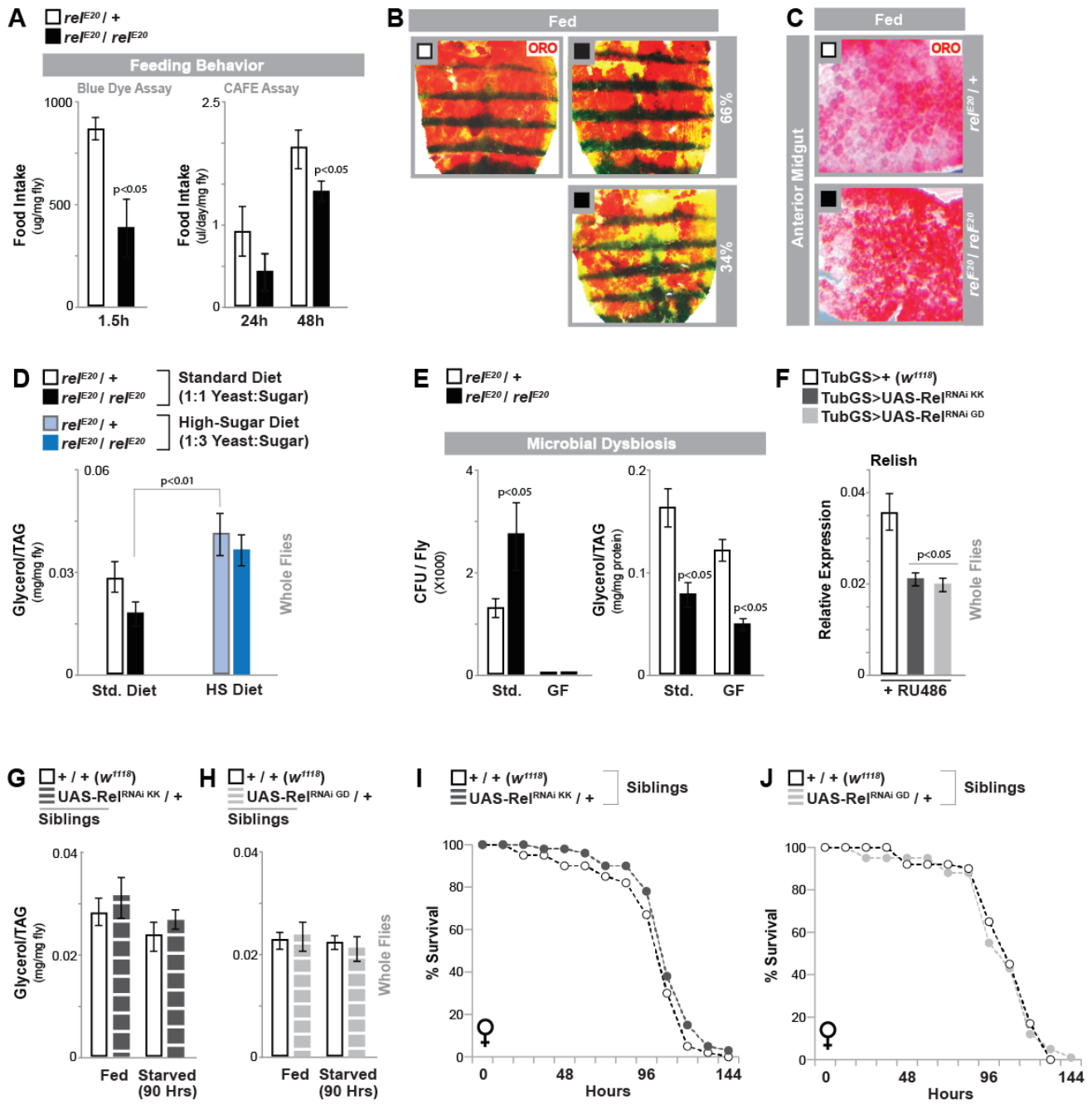


Figure S2

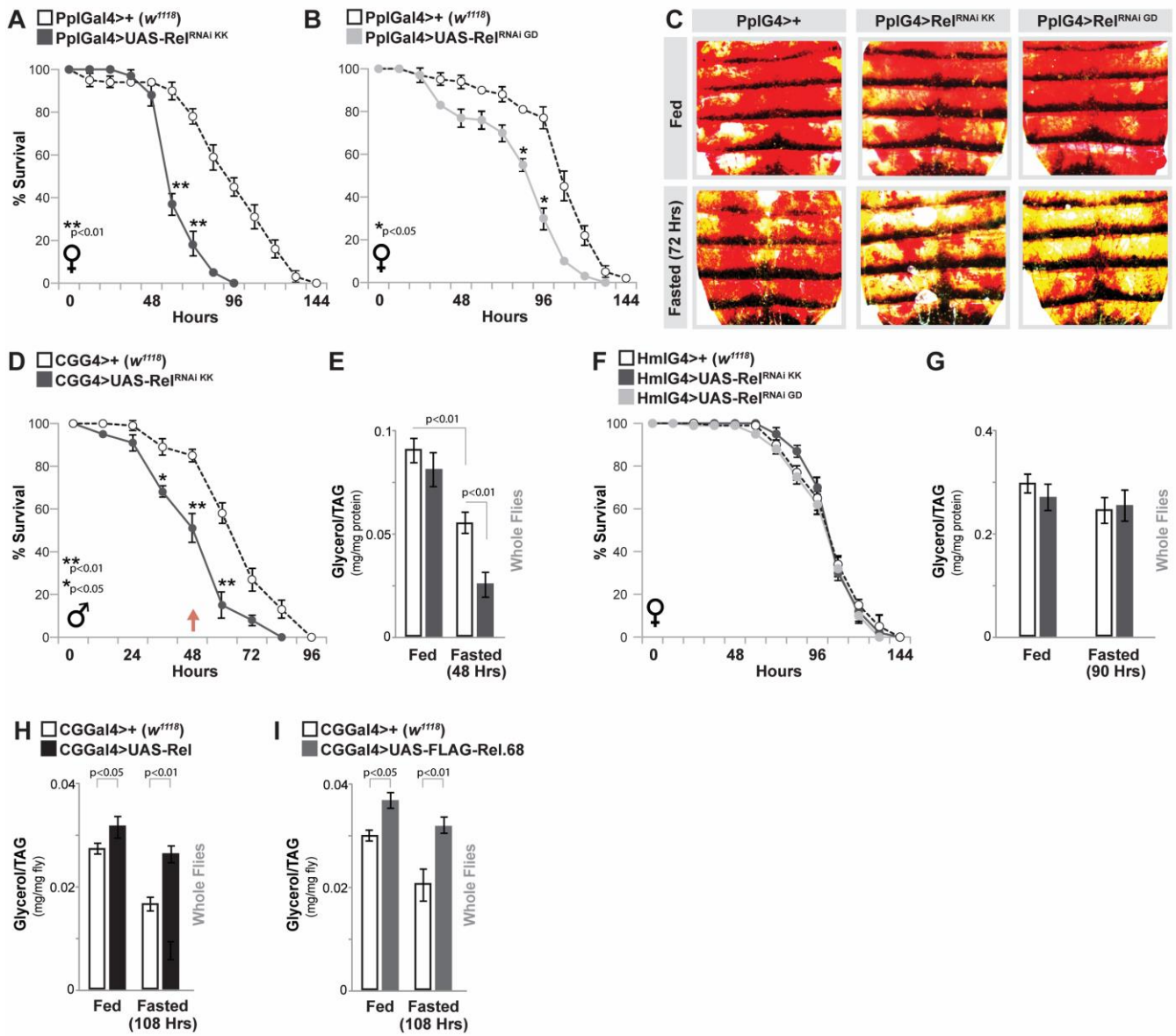


Figure S3

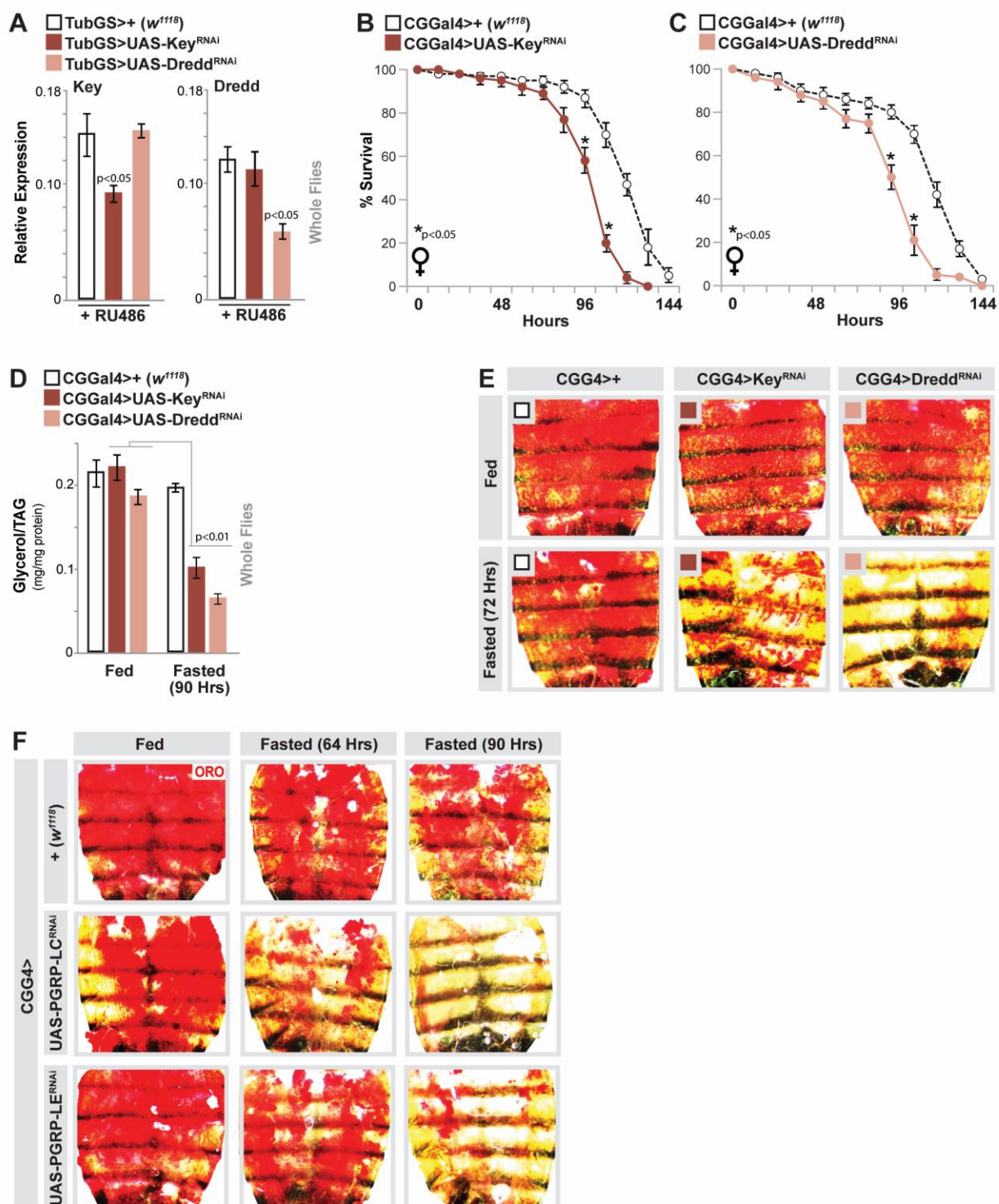


Figure S4

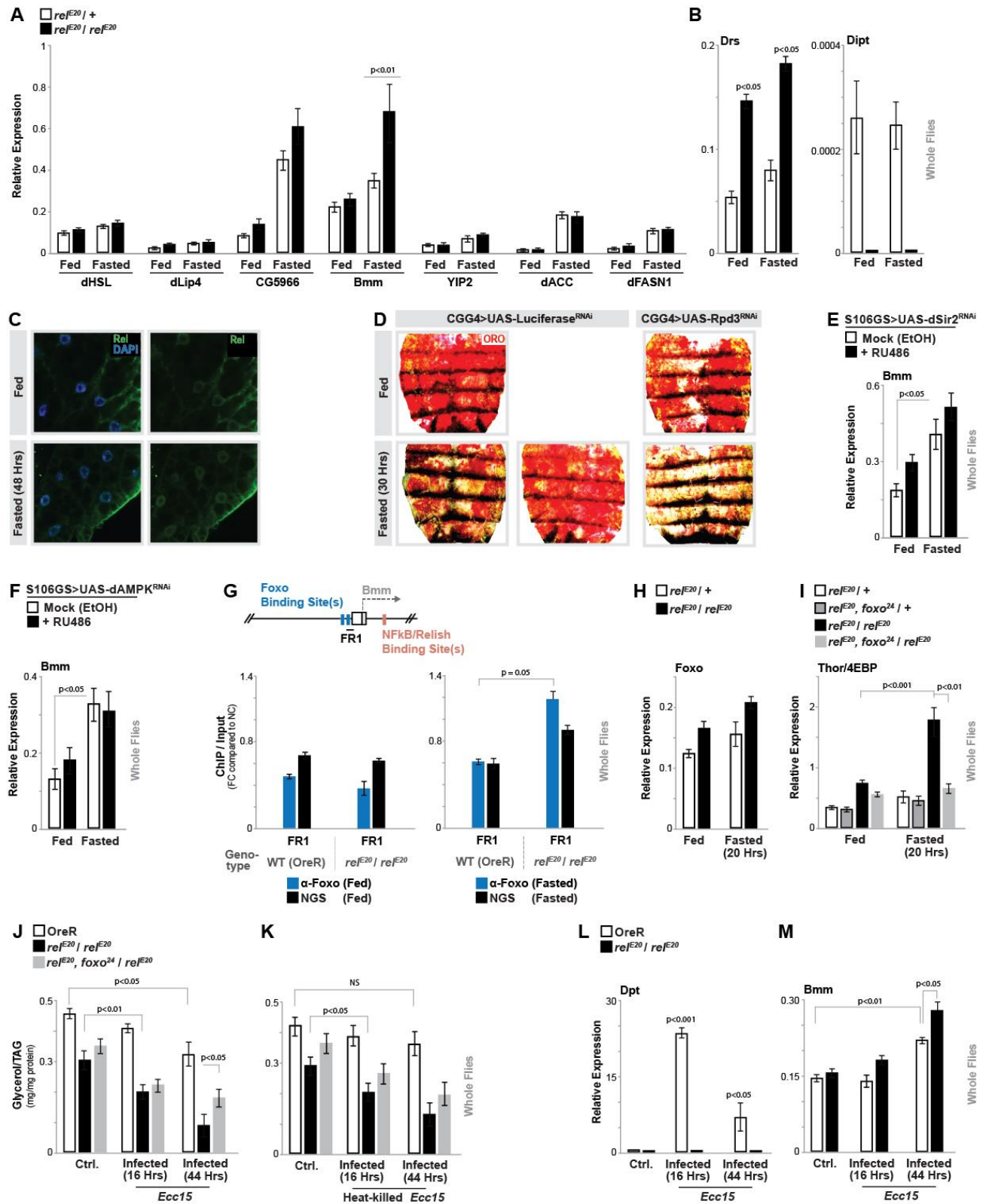


Figure S1: NF- κ B /Relish-dependent changes in organismal lipid homeostasis. Related to Figure 1.

(A) Relish-dependent changes in feeding behavior. *relE20/relE20* (mutant) female flies display decreases in food intake using both the Blue Dye feeding assay (n=3-6 cohorts of 5 flies, measured ZT(8-10) after 1.5 hours feeding) and the CAFE assay (n=7 samples measured after 24 hours and 48 hours); compared to *relE20/+* controls. Note: *relE20/relE20* mutant show stronger decreases in acute food intake (Blue Dye, 1.5 hours) as opposed to chronic (CAFE, 48 hours).

(B-C) Oil red O (ORO) neutral lipid stain in dissected (B) fat body/carcass and (C) intestine from *relE20/relE20* (mutant) female flies compared to *relE20/+* control flies. Images from intestine taken from anterior midgut. Note: *relE20/relE20* mutant show variable decreases in lipid storage in fat body, but not in the intestine. Percentages represent relative contribution of mild (top panel) or strong (bottom panel) lipid storage defects from 45 unique fat body/carcass dissections from multiple, independent experiments.

(D) Relish-dependent (*relE20/relE20* mutant) changes in total triglyceride (TAG) levels (whole flies) during *ad libitum* feeding (compared to *relE20/+* controls) can be minimized by feeding a high calorie/high sugar diet (n = 5 samples).

(E) Relish-dependent changes in triglyceride levels during *ad libitum* feeding are not caused by microbial dysbiosis. Colony forming units (CFU per fly, n = 4) and total triglyceride (TAG) levels of whole flies (n = 4 samples) in standard rearing conditions (Std.) or germ-free rearing conditions (GF); genotypes *relE20/+* (control) or *relE20/relE20* (mutant).

(F) UAS-Rel RNAi efficiency. Changes in *relish* transcription (measured by qRT-PCR in whole flies) upon ubiquitous Relish depletion (RNAi line v108469-KK and v49413-GD) using Tubulin-GeneSwitch-Gal4 (TubGS) after 5 days feeding RU486; compared to controls (TubGS>+(w¹¹¹⁸)). n = 4 samples.

(G-J) UAS-Rel RNAi transgenes (RNAi lines v108469-KK and v49413-GD) alone do not affect fasting-induced triglyceride metabolism or survival during metabolic adaptation. (G-H) Total TAG levels of whole female flies (n=5 samples, before and after fasting (90 hours)) and (I-J) starvation resistance of female flies (n = 5 cohorts, total 89-96 flies) from UAS-Rel RNAi/+(w¹¹¹⁸) and +/+(w¹¹¹⁸) female siblings.

All bars and line graph markers represent mean \pm SE. All flies were 7 days old post-eclosion.

Figure S2: NF- κ B/Relish-dependent changes in lipid metabolism in response to metabolic adaptation. Related to Figure 1.

(A-C) Changes in lipid metabolism and survival upon Relish depletion (RNAi lines v108469-KK and v49413-GD) in fat body (PplGal4). (A-B) Starvation resistance of female flies. n = 6 cohorts (total 110-141 flies). (C) Oil Red O (ORO) neutral lipid stain of dissected carcass/ fat body before and after fasting (72 hours).

(D-E) Changes in lipid metabolism and survival upon Relish depletion (RNAi lines v108469-KK) in fat body (CGGal4) of male flies. (D) Starvation resistance of male flies. n = 5 cohorts (total 90-95 flies). (E) Total triglyceride (TAG) levels of whole male flies (n=5 samples, before and after fasting (48 hours)).

(F-G) Absence of changes in lipid metabolism and survival upon Relish depletion (RNAi lines v108469-KK and v49413-GD) in hemocytes (HmlGal4) of female flies. (F) Starvation resistance of female flies. n = 4 cohorts (total 77-80 flies). (G) Total triglyceride (TAG) levels of whole male flies (n=3 samples, before and after fasting (90 hours)).

(H-I) Changes in fasting-induced lipid metabolism upon Relish over-expression (both (H) full-length Relish (UAS-Rel) and (I) the tagged N-terminal active fragment (UAS-FLAG-Rel.68)) in fat body (CGGal4). Total TAG levels of whole female flies (n=5 samples, before and after fasting (108 hours)). Control genotype CGGal4/+ (w^{1118}).

Bars and line graph markers represent mean \pm SE. All flies were 7 days old post-eclosion.

Figure S3: Kenny and Dredd-dependent changes in lipid metabolism in response to metabolic adaptation. Related to Figure 1 and 3.

(A) RNAi efficiency. Changes in *kenny* or *dredd* transcription (measured by qRT-PCR in whole flies) upon ubiquitous depletion (Kenny (Key) RNAi line v7723-GD and Dredd RNAi line v104725-KK) using Tubulin-GeneSwitch-Gal4 (TubGS) after 5 days feeding RU486; compared to controls (TubGS>+ (w^{1118})). n = 4 samples.

(B-E) Changes in lipid metabolism and survival upon Kenny or Dredd depletion (RNAi lines v7723-GD (Key) and v104726-KK (Dredd)) in fat body (CGGal4) of female flies. (B-C) Starvation resistance of female flies. n = 7 cohorts (total 140-149 flies). (D) Total triglyceride (TAG) levels of whole female flies (n=5 samples, before and after fasting (90 hours)) and (E) Oil Red O (ORO) neutral lipid stain of dissected carcass/ fat body before and after fasting (72 hours). Control genotype CGGal4/+ (w^{1118}).

(F) Changes in lipid metabolism upon PGRP-LC or PGRP-LE depletion (RNAi lines v101636-KK (LC) and v23664-GD (LE)) in fat body (CGGal4) of female flies. Oil Red O (ORO) neutral lipid stain of dissected carcass/ fat body before and after fasting (64 and 90 hours). Control genotype CGGal4/+ (*w*¹¹¹⁸).

Bars and line graph markers represent mean \pm SE. All flies were 7 days old post-eclosion.

Figure S4: Fasting-induced and NF- κ B/Relish-dependent changes in gene expression and transcriptional regulation. Related to Figure 3-4.

(A) *Drosophila* *HSL*, *lip4*, *CG5966*, *bmm*, *YIP2* (yippee interacting protein 2/thiolase), *ACC* (acetyl-CoA carboxylase), and *FASN1* (fatty acid synthase) transcription (measured by qRT-PCR in whole flies) before and after fasting (20 hours). *relE20/+* (heterozygote control), or *relE20/relE20* (mutant) genotypes. n = 3 samples.

(B) *Drosophila* *drs* (Drosomycin) and *dipt* (Diptericin) transcription (measured by qRT-PCR in whole flies) before and after fasting (20 hours). *relE20/+* (heterozygote control), or *relE20/relE20* (mutant) genotypes. n = 4 samples.

(C) Relish immunostaining in carcass/fat body before and after fasting (20 hours; OreR female flies). Stained with anti-Rel and nuclei visualized with DAPI (blue). Weak Rel signal is detected in the nucleus during fed and fasted conditions, however, the staining is slightly more perinuclear during *ad libitum* feeding (upper right panel).

(D) Changes in lipid metabolism upon Rpd3 depletion (RNAi TRiP 36800) in fat body (CGGal4) of female flies. Oil Red O (ORO) neutral lipid stain of dissected carcass/ fat body before and after fasting (30 hours). Control genotype CGGal4>UAS-Luciferase RNAi (slight variation in control phenotype after fasting is highlighted with two independent images).

(E-F) Changes in *bmm* transcription (measured by qRT-PCR in whole flies) upon fat body-specific depletion of *Drosophila* (E) AMPK α (RNAi line v1827-GD) and (F) Sir2 (homolog of SIRT1; dSir2 RNAi line v23201-GD) using S106-GeneSwitch-Gal4 after 5 days feeding RU486; compared to controls (mock (EtOH) treated siblings) before and after fasting (90 hours). n = 4-5 samples.

(G) Schematic shows *Bmm* locus (focusing on the upstream promoter and first intron proximal to transcription start site), as well as Foxo and NF- κ B/Rel binding motifs. FR1 represents regional target site of Foxo binding (and corresponding primer set) tested in ChIP-qPCR analysis. The histogram represents ChIP-qPCR analysis of Foxo binding to the *Bmm* promoter/locus in fed (left panel) and fasted (20 hours; right panel) conditions. ChIP-qPCR

analysis with normal goat serum (NGS) is included as a control. Plotted as fold change (FC) of indicated PCR primer sets compared to a negative control (NC) primer set. n = 3 samples.

(H) *Drosophila foxo* transcription (measured by qRT-PCR in whole flies) before and after fasting (20 hours). *relE20/+* (heterozygote control), or *relE20/relE20* (mutant) genotypes. n = 3 samples.

(I) Relish-Foxo antagonism controls Thor/4EBP expression during fasting. *Drosophila thor* (homolog of 4EBP) transcription (measured by qRT-PCR in whole flies) before and after fasting (20 hours) in controls (*relE20/+* and *relE20, foxo24/+*), mutant (*relE20/relE20*) and mutant with reduction in Foxo gene dose (*relE20, foxo24/relE20*) genotypes. n = 3 samples.

(J-K) Changes in lipid metabolism (total triglyceride (TAG) levels of whole female flies) after systemic *Ecc15* infection with (J) live or (K) dead bacteria (16 and 44 hours post infection) in controls (OreR), mutant (*relE20/relE20*), and mutant with reduction in Foxo gene dose (*relE20, foxo24/relE20*) genotypes. n=3-5 samples. TAG levels decline after acute (16 hours) and chronic (44 hours) infection with live bacteria in Relish mutant flies, while slight TAG level changes in controls are observed only after 44 hours. Reducing gene dose of Foxo in Relish mutant flies partially rescues the accelerated loss of TAG levels only 44 hours post-infection. Treatment with dead bacteria drive similar, but slightly attenuated, changes in TAG levels, suggesting that the presence of live bacteria may impinge different energy demands on the host that shape metabolic adaptation in response to infection.

(L-M) Changes in (L) *Dpt* and (M) *bmm* transcription (measured by qRT-PCR in whole flies) before and after systemic *Ecc15* infection (16 and 44 hours post infection) in controls (OreR) and mutant (*relE20/relE20*) genotypes. n = 3-4 samples. *bmm* transcription is slightly elevated after chronic systemic infection in controls (44 hrs, as *Dpt* transcription begins to subside) and is further enhanced at this time-point in Relish mutant flies.

Bars represent mean \pm SE. All flies were 7 days old post-eclosion.

	Forward	Reverse
qRT-PCR Primers		
Relish	CATCAGGAGACAGAGCGTGA	CCGACTTGCGGTTATTGATT
Kenny	TGACAAGGTCAACCAAACCA	CCTGCTCCTTTAGCCTGATG
Dredd	CAGGAGATCCACTTCGCTTC	CGACTGCTGGTTATCCGATT
Brummer	CAATAAGGGTCTGGCCAACTGGAT	TAAGTCCTCCACCATTACTCTGGC
dHSL	ATGAGTGGCTTTCCCAACTG	CATGGCTTCGTTGGATAACA
dLip4	TGGATAGCTCAGCCACTT	GCGGGTATATCATGCTTTCC
CG5966	CTGCAATCACATTCGCAGTC	TGCTCCTGGTAATCCTCCTG
YIP2	CGGTCTTAAGGGTGAGCAA	ACATTACGGGCAATGAAAGG
dACC	CTATCGCTATGGTTACCTGCCGTA	AACATGATCTGTGTGCCACCCAA
dFASN1	TGATGGCCGGTATTCTGGAAGAGA	ATTGCTCATCAGCTCAGCGAACCT
Dipt	TTCATTGGACTGGCTTGTGCCTTC	TGAGGCTCAGATCGAATCCTTGCT
Drs	AAGTACTTGGCCCTCTTCGCT	TCCTTCGCACCAGCACTTCAGACT
Foxo	TCTCGCCGAACTCAGTAACC	CCTCCAGGCATTGTCCTATC
Thor	CACTTGCGGAAGGGAGTACG	TAGCGAACAGCCAACGGTG
Actin5c	CTCGCCACTTGCCTTACAGT	TCCATATCGTCCCAGTTGGTC
ChIP-qRT-PCR Primers		
R1 (Bmm locus)	GCTTGTTTGCCTTTGTAGGTC	TTCGAAATTGGACAAACACG
R2 (Bmm locus)	TGTCGCTGACAATCAAAGC	TTCTGGGTGGAGTTTGGAAC
Act5c ^P	AACCCCAAATTGAATCACA	GAGAATTCCTCCGCAACTG
Dipt ^P	AAGAAAGATCCCCTGGTGGT	TTTTATAGGCCGCTTTCCAA
FR1 (Bmm locus)	CACCGCGCCGCAATGAATGTATAA	TTCAATCACTGTTTGTGCGGTCGGC

Table S1: Primer sequences used for qRT-PCR (related to Figures 2, 3, 4, S1, S3, and S4)